Role of quasiresonant planetary wave dynamics in recent boreal spring-to-autumn extreme events

Vladimir Petoukhov[a,1], Stefan Petri[a], Stefan Rahmstorf[a], Dim Coumou[a], Kai Kornhuber[a], and Hans Joachim Schellnhuber[a,b,1]

[a]Potsdam Institute for Climate Impact Research, D-14412 Potsdam, Germany; and [b]Santa Fe Institute, Santa Fe, NM 87501

Contributed by Hans Joachim Schellnhuber, May 4, 2016 (sent for review July 15, 2015); reviewed by Rasmus E. Benestad and David Karoly)

In boreal spring-to-autumn (May-to-September) 2012 and 2013, the Northern Hemisphere (NH) has experienced a large number of severe midlatitude regional weather extremes. Here we show that a considerable part of these extremes were accompanied by highly magnified quasistationary midlatitude planetary waves with zonal wave numbers m = 6, 7, and 8. We further show that resonance conditions for these planetary waves were, in many cases, present before the onset of high-amplitude wave events, with a lead time up to 2 wk, suggesting that quasiresonant amplification (QRA) of these waves had occurred. Our results support earlier findings of an important role of the QRA mechanism in amplifying planetary waves, favoring recent NH weather extremes.

weather extremes | heat waves | waveguides | planetary waves | atmospheric dynamics

Recent years have seen an increasing number, severity, and spatial scale (covered area) of summer extremes in the Northern and Southern Hemispheres (NH and SH), such as the European heat wave in 2003, the Russian heat wave and the Indus river flood in Pakistan in 2010, and the heat waves in the United States in 2011 (1–3). Model projections suggest that weather extremes may become even more intense, more frequent, and longer in the climate of the future (4). Several conceptual mechanisms have been proposed to explain the physical basis of the extremes and the reason for the increase in their frequency of occurrence.

As shown by Coumou et al. (5) and Comou and Robinson (6), the observed long-term increase in frequency of extreme heat events can, on a global scale, be explained purely thermodynamically as a response to a shift in the mean surface temperatures to warmer values. Likewise, general trends toward higher annual maximum daily rainfall are consistent with an overall rise in atmospheric moisture associated with warmer air (7–9).

Recent global climate change is also likely to affect large-scale atmospheric circulation patterns, with strong nonlinear feedbacks between thermodynamic and dynamic components of the climate system (10, 11). This could potentially alter the frequency of extremes on seasonal to subseasonal timescales. In one of the first studies on this issue, Schär et al. (12) developed a stochastic concept of regional blocking events for the explanation of the 2003 European heat wave as a result of the observed climatic warming trend, which shifts and widens the probability distribution of summer temperatures. Luterbacher et al. (13) estimated a return period for this type of extreme event as being about 100 y in the European region, taking climatic warming into account. However, a number of severe summer extremes have already occurred since then in the NH, particularly in Europe. The anomalous atmospheric circulation patterns accompanying these extremes were of hemispheric scale (14–22). They encircled the entire NH and persisted over nearly the whole summer, which is fundamentally different from conventional regional blocking events with about a 10-d life span (23). This shows that not only purely stochastic regional mechanisms of extremes are at work (3). Based on the NH annular mode (NAM) (see ref. 24), Tachibana et al. (14) showed that an anomalously strong positive summer NAM (as occurred specifically during the 2003 European heat wave) accounted well for hemispheric weather regimes with anomalously high midlatitude blocking activity between strongly marked polar and subtropical jets, over the period 1958–2005. Black et al. (15) analyzed basic factors that likely contributed to the summer 2003 European heat wave, examining large-scale atmospheric flow, regional heat budget at the top of the atmosphere, and sea surface temperature. As a key factor, the authors of ref. 15 identified a Rossby wave train of alternating-sign stream function anomalies, spreading northnortheast from the source region in tropical America across the Atlantic and farther into Eurasia. This pattern resembles those discussed conceptually in ref. 25. Similar to ref. 15, Cassou et al. (16) argue that the anomalously warm June 2003 in western Europe could be related to wetter-than-average conditions in the Caribbean that triggered the occurrence of a Rossby wave train pattern stretching from the Caribbean across the Atlantic, whereas the anomalous August 2003 could be associated with a summer NAO-like pattern and enhanced monsoon over the Sahel, which might have been compensated dynamically by anomalously strong downdrafts over Europe. Hong et al. (17) and Lau and Kim (18) described a Rossby wave train spanning Eurasia during the catastrophic 2010 Pakistan flood and Russian heat wave, with the southern branch spreading through northern Pakistan and being accompanied by heavy monsoon surges there.

Branstator (26) proposed a mechanism of generation of predominantly zonally oriented Rossby wave trains. He showed that a sufficiently intense quasizonal subtropical jet could act as a waveguide for a quasistationary zonal wave number 5. The mechanism

Significance

Weather extremes are becoming more frequent and severe in many regions of the world. The physical mechanisms have not been fully identified yet, but there is growing evidence that there are connections to planetary wave dynamics. Our study shows that, in boreal spring-to-autumn 2012 and 2013, a majority of the weather extremes in the Northern Hemisphere midlatitudes were accompanied by highly magnified planetary waves with zonal wave numbers *m* = 6, 7, and 8. A substantial part of those waves was probably forced by subseasonal variability in the extratropical midtroposphere circulation via the mechanism of quasiresonant amplification (QRA). The results presented here support the overall hypothesis that QRA is an important mechanism driving many of the recent exceptional extreme weather events.

Author contributions: V.P. and H.J.S. designed research; S.R., D.C., and K.K. performed research; S.P. and K.K. analyzed data; and V.P. and S.R. wrote the paper.

Reviewers: R.E.B., The Norwegian Meteorological Institute; and D.K., University of Melbourne.

The authors declare no conflict of interest.

Freely available online through the PNAS open access option.

[1]To whom correspondence may be addressed. Email: john@pik-potsdam.de or petukhov@pik-potsdam.de.

This article contains supporting information online at www.pnas.org/lookup/suppl/doi:10.1073/pnas.1606300113/-/DCSupplemental.

was subsequently applied to explain several important features of some of the recent summer extremes (18–21, 27).

Francis and Vavrus (28) have suggested a conceptual model of deceleration and increase in the north–south meridional extent of eastward-propagating midlatitude planetary Rossby waves over the North America/North Atlantic sector caused by the recently observed decrease in the midlatitudinal westerly winds. In their study, these authors rely on observational evidence of recent Arctic amplification (AA), i.e., a strong increase in lower-tropospheric temperatures in the Arctic compared with that over the total NH (see, e.g., ref. 29). The authors of ref. 28 hypothesized that AA, consistent with polar sea ice loss, might favor a decrease in midlatitude westerlies and therefore lead to increased probabilities of persistent extreme regional weather events in the NH midlatitudes. At least in summer, the NH westerlies and storm tracks have really weakened over 1979–2015 (30, 31).

Screen (32) explored the influence of Arctic sea ice on European summer climate using a state-of-the-art atmospheric model in view of the historically unprecedented sequence of six consecutive wet summers from 2007 to 2012 in northern Europe, which featured a marked southward shift of the polar jet stream. He found that prescribed sea ice loss in the model caused a southward shift of the summer jet stream and increased northern European precipitation. An anomalous Rossby wave-4 train is reported by Hanna et al. (33), when studying the exceptional Greenland ice sheet melt in summer 2012.

Petoukhov et al. (34) proposed a common mechanism for generating persistent high-amplitude quasibarotropic planetary-scale wave patterns of the NH midlatitude atmospheric circulation with zonal wave numbers $m = 6$, 7, and 8 that can explain a number of the major NH summer extremes over the 1980–2011 period (34, 35). Petoukhov et al. (34) showed that these patterns could result from the trapping of free quasistationary barotropic Rossby waves with zonal wave numbers k equal or close to the three integer values indicated above, within the predominantly zonally oriented midlatitude waveguides. Unlike the one considered in Branstator (26) for zonal wave number 5, the formation of these waveguides is based on a specific change in the latitudinal shape (and not the magnitude) of the quasizonal extratropical winds at the equivalent barotropic level (EBL). The midlatitude waveguides considered in ref. 34 can favor an onset of midlatitude quasiresonant amplification (QRA) of these waves, causing a strong increase in the atmosphere's dynamical response to quasistationary midtroposphere external forcing with zonal wave numbers $m = 6$, 7, and 8 (*Calculation of the Meridional Wave Number*). The reason for the change in the shape and positions of atmospheric jet streams is, for now, an issue of debate, with AA as one of the potential candidates (see, e.g., refs. 36 and 37).

Recently, Screen and Simmonds (38) showed that, during 1979–2012, months with extreme weather (in terms of high anomalies of land surface temperature and land precipitation) in the NH midlatitudes were commonly accompanied by zonally elongated midlatitude trains of quasistationary midtropospheric planetary waves, predominantly with $m = 5–7$. Their findings also suggest that amplified quasistationary waves with these wave numbers increased the probabilities of extreme weather events over the NH midlatitudes.

QRA Mechanism of Planetary Wave Reinforcement presents a brief description of the QRA mechanism proposed in ref. 34. In *Spring to Autumn Weather Extremes*, we investigate, within the framework of QRA, severe regional weather extremes that occurred in boreal spring-to-autumn 2012 and 2013 in the NH. We show that a considerable portion of these extremes could be favored by QRA events for the midlatitude waves with zonal wave numbers 6, 7, and 8. In *Discussion*, we discuss the results presented in *Spring to Autumn Weather Extremes* and briefly touch on the issue of high-amplitude quasistationary midlatitude waves with zonal wave numbers 4 and 5.

QRA Mechanism of Planetary Wave Reinforcement

Rossby waves (also known as planetary waves) are ubiquitous in ocean and atmosphere. In the atmosphere, we can distinguish forced and free Rossby waves. Forced Rossby waves occur as a response of the midtroposhere and high-troposphere atmospheric circulation to the external diabatic and orographic forcing (25, 39, 40), which arises, e.g., from the thermal contrast between land and oceans as well as from mountain ranges. They occur at various wave numbers and are quasistationary and principally barotropic. Free extratropical Rossby waves with zonal wave numbers about 6 to 8 mostly occur as high-amplitude, fast traveling waves (the so-called synoptic transients responsible for much of the weather variability in the extratropics); once established, they can freely propagate predominantly to the east with a phase speed $c \approx 6–12$ m·s^{-1} without maintenance from external forcing. In contrast to these fast traveling waves, the quasistationary extratropical barotropic free waves with zonal wave numbers 6 to 8 are normally weak, with a magnitude of the meridional wind velocity less than 1.5–2.5 m·s^{-1} (25, 34, 35, 39, 40).

However, using National Centers for Environmental Prediction –National Center for Atmospheric Research (NCEP-NCAR) reanalysis data (41), Petoukhov et al. (34) showed that, during a number of recent NH extremes in July and August, certain persistent high-amplitude atmospheric wave patterns with barotropic vertical structure evolved, to which the quasistationary component of midlatitude barotropic free waves with zonal wave numbers $k \approx 6–8$ made an exceptionally large contribution. These authors also presented an explanation for the emergence of these unusual high-amplitude wave patterns, namely that they were due to the mechanism of QRA of planetary waves.

In ref. 34, the QRA mechanism is applied to quasistationary and circumglobal planetary waves, i.e., those that wrap around the planet in the midlatitudes. These waves are solutions to the full wave equation, including forcing, for integer values of the zonal wave number m (we will refer to them as m waves). This corresponds to the solutions of the forced oscillator, with m as the analog of the frequency of the external force. In addition, there are also solutions to the homogeneous wave equation (without forcing terms), i.e., free waves. These waves with zonal wave numbers $k \approx 6–8$ (they can be noninteger; we will call these waves k waves) usually experience strong meridional dispersion, and, for that reason, their energy disperses rapidly. However, under specific conditions, two strongly reflecting points [the so-called turning points (TPs)] can emerge for these waves in the midlatitudes, at which the square of their meridional number, l^2, changes sign, with $l^2 > 0$ between the TPs. This leads to the development of a waveguide for these free waves, which traps them in the midlatitudes and prevents their strong dispersion, with the location of the southern and northern boundaries of the waveguide closely related to the position of the TPs. Planetary waves with these wave numbers thus become the favored free waves of the system, analogous to the natural frequency of an oscillator. Then, in cases where these favored free k-wave numbers are close to those of the m waves pushed by the forcing, i.e., if k is close to m, a resonance can arise resulting in large m-wave amplitudes, analogous to the forced oscillator when the frequency of the external force is close to the natural frequency (34).

Whether a waveguide develops for a particular wave number k depends on the latitudinal shape of the zonal mean midtroposphere zonal winds $\overline{u}$ in the extratropical atmosphere. The equations for Rossby waves (*Calculation of the Meridional Wave Number*, *Physics of the Parameter*, and *Calculation of the Amplitudes*) show that this can occur if a set of necessary conditions are met: $\overline{u} > 0$ in the midlatitude region; the highest value of l within the waveguide is in the range of the meridional wave numbers l_m dominantly contributing to the external forcing with a given m, which provides closeness of the k waves to respective m waves

not only in terms of the zonal but also the meridional wave numbers, favoring the QRA of the m waves; the total latitudinal width of the waveguide is no less than the characteristic spatial scale of the relevant Airy function (25), which is used as the boundary condition at its southern and northern boundaries; and latitudinal distribution of l is sufficiently smooth in the waveguide, and both TPs lie within a midlatitude region of ~ 25°N–30°N and ~65°N–70°N, as the necessary condition for the application of quasilinear Wentzel–Kramers–Brillouin (WKB) method (25) when solving the equations for Rossby waves. The above necessary conditions for QRA are combined in ref. 34 in a set of four necessary conditions *i*–*iv* that are discussed in the main text and supporting information of that paper (see also *Basic Necessary Conditions and Assumptions* for details).

In this paper, we deal with the 15-d running means over May–September of the studied waves. In that case, the amplitude, $\tilde{A}_m^{Ort}$, of the m component of the midlatitude external forcing experiences generally noticeably higher variations in time, compared with those of monthly means investigated in ref. 34. In view of this, we pose here an additional necessary condition that the minimum value of $\tilde{A}_m^{Ort}$ should exceed some threshold number, $\tilde{A}_{m,\min}^{Ort}$, allowing us to use the quasilinear WKB method when solving the equations for the studied Rossby waves (see *Additional Necessary Condition of the Minimum Amplitude*).

In the 15-d running means of the m waves, we have situations (very rare, however) of coexistent, closely adjacent, or even overlapping in latitude, midlatitude waveguides, each satisfying all of the above-mentioned necessary conditions of QRA, with, however, low amplitudes of the observed m waves triggered within up to 2 wk. The analysis of the results shows that, in all those cases, the distance between the adjacent boundaries of the waveguides is lower than the characteristic spatial scale of the relevant Airy functions. This presumably violates a high reflection of the wave energy at these boundaries, causing, instead, a noticeable interaction, including the nonlinear interference, between the m waves trapped in the waveguides. We exclude all those cases from our consideration, posing an additional necessary condition on the minimum allowable distance between multiple coexisting waveguides (see *Additional Necessary Condition Posed* for details).

When all of the above necessary conditions for quasiresonance are met, then the QRA amplitude, $\tilde{A}_m$, for the meridional velocity in the midlatitude m wave at the EBL is described in dependence on the thermal and orographic forcing amplitude $\tilde{A}_m^{Ort}$ at this level (*Calculation of the Amplitudes*) by the following equation (see equation S14 in ref. 34):

$$\tilde{A}_m = \frac{\tilde{A}_m^{Ort}}{\left\{\left[(k/a)^2-(m/a)^2\right]^2 + C_{1,m}^2\left(L/a^2+Ro^2/L\right)^2(m/a)^2\right\}^{1/2}}. \quad [1a]$$

In Eq. **1a**, a is the Earth's radius, and L and Ro are, respectively, the characteristic Rossby radius and Rossby number for the eddies contributing effectively to atmospheric near-surface and internal "eddy friction" described by the second term in curly braces in the denominator of the right-hand side of Eq. **1a** (*Calculation of the Meridional Wave Number*). A nondimensional parameter $C_{1,m} \geq 0$ in Eq. **1a** represents the ratio of the zonally averaged module of the geostrophic wind at the top of the planetary boundary layer to that at the EBL, $\bar{u}$ (34) (see *Physics of the Parameter* for more detail).

As follows from Eq. **1a**, in the absence of atmospheric friction, a classic resonance takes place, with $\tilde{A}_m \to \infty$ if $k \to m$, whereas, for realistic values of L, Ro, and $C_{1,m}$, $\tilde{A}_m$ reaches a high but finite quasiresonant value if $k = m$. This is the essence of the QRA mechanism of the planetary wave reinforcement proposed in ref. 34. QRA can be regarded as an extension of the Haurwitz-type mechanism (42) of a strong increase in the amplitude of the midlatitude atmospheric barotropic wave system response to stationary external barotropic thermal forcing, with a spatial frequency m approaching the natural stationary spatial frequency k of the wave system, to the case of external barotropic thermal and orographic forcing under a latitude-dependent $\bar{u}$ and an integer m over the midlatitude belt on the spherical Earth.

In the present paper, unlike ref. 34, in some rare cases, the QRA amplitudes $\tilde{A}_m$ of the 15-d running means calculated by Eq. **1a** reached very high values about 10–15 m·s^{-1}. On the other hand, the theory of the wave breaking process in the middle and high atmosphere, which is the basic one limiting $\tilde{A}_m$ from above in the extratropics (see, e.g., ref. 43), requires substantially lower values of the amplitudes of the considered m waves. Following this requirement, we assign the maximum allowable value for $\tilde{A}_m$, $Ag(m)$, the latter being the amplitude of the m wave in the process of wave breaking (43) (see *Amplitude of Wave Breaking*), so that, if $\tilde{A}_m$ calculated by Eq. **1a** exceeds $Ag(m)$, we put

$$\tilde{A}_m = Ag(m). \quad [1b]$$

We note that this condition does not present an additional necessary condition of QRA but rather just limits the predicted wave amplitude in cases of resonance.

The theory of QRA, based on the equations for Rossby waves, thus allows us to specify the necessary conditions under which a QRA of planetary waves can occur. The explanatory power of QRA theory can only be established empirically, by comparing the times of resonance conditions and the estimated amplitudes to the high-amplitude waves actually observed. This will be done in this paper.

Spring-to-Autumn Weather Extremes 2012 and 2013 in the Context of QRA

In this paper, we extend the investigation of recent NH regional extremes in the framework of QRA to the years 2012 and 2013. These years are marked by a large number of strong regional extremes in the NH during May–September (see, e.g., refs. 44 and 45). We show that a considerable number of these extremes could have been favored by the QRA mechanism proposed in ref. 34, as was shown there for many July–August extremes observed during the last three decades. Fig. 1 displays the time series of a standard planetary wave diagnostic, namely the observed wave amplitudes $\tilde{A}_{m,obs}$ over May–September 2012 and 2013 of the 15-d running means for zonal wave numbers $m = 6$, $m = 7$, and $m = 8$ of the meridional wind velocity at 300 hPa averaged over the 37.5°N–57.5°N latitude range, diagnosed from daily NCEP-NCAR reanalysis data (41). As shown in ref. 34, 15-d running means of the studied waves meet the condition of quasistationarity, with the characteristic values of longitudinal phase velocity about 1–2 m·s^{-1}. As seen from Fig. 1, there occurred 17 high-peak-amplitude (HPA) events (see the set of filled and open circles in Fig. 1), with amplitudes exceeding 1.5 SDs above the 1980–2013 climatology. Of these events, nine occurred in 2012 and eight occurred in 2013; 13 of the 17 HPA events marked by filled circles in Fig. 1 occurred within up to 2 wk of QRA events, i.e., times during which all of the necessary conditions for QRA were satisfied and the amplitudes $\tilde{A}_m$, calculated with the use of Eqs. **1a** and **1b** (predicted QRA amplitudes), exceeded 1.5 SDs above the corresponding 1980–2013 climatology (see Fig. 1). These QRA amplitudes are marked by filled squares in Fig. 1. As seen from Fig. 1, $\tilde{A}_m$ are in a good agreement with the observed amplitudes $\tilde{A}_{m,obs}$ of respective HPA events.

In 12 of these 13 cases, the quasiresonance conditions (QRA event) preceded or occurred substantially simultaneously with the respective HPA event (we call it a combined QRA–HPA

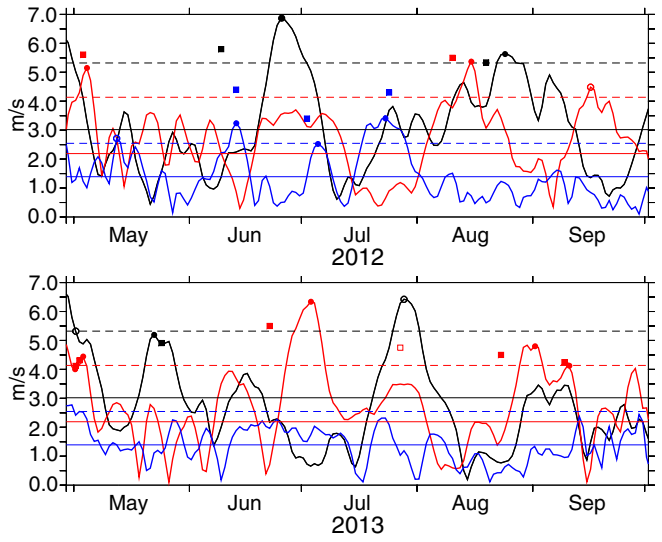

Fig. 1. Time series of the observed amplitudes (in meters per second) of zonal wave numbers $m = 6$ (black), $m = 7$ (red), and m = 8 (blue) for the 15-d running means of the meridional wind velocity at 300 hPa averaged over 37.5°N–57.5°N for May–September 2012 and 2013, based on daily reanalysis data (41). The filled circles designate the observed HPA events exceeding the 1.5 SD (dashed horizontal lines) above the 1980–2013 climatology (solid horizontal lines), when the QRA mechanism was at work within up to 1.5–2 wk time offset relative to respective HPA event. The amplitudes of these QRA events are marked by colored filled squares. The open circles denote the observed HPA events when the QRA mechanism was not in action. The open square marks the high amplitude of the QRA event for $m = 7$, when the corresponding QRA-predicted HPA event did not happen.

event), supporting a causal link. According to refs. 44 and 45, severe NH midlatitude regional extremes occurred in connection with these QRA–HPA events.

A large number of HPA events over May–September (nine in 2012 and eight in 2013) for the waves with $m = 6$, 7, and 8 is typical for the years with the most severe extremes in the NH midlatitudes, e.g., 2003, 2006, and 2010, with 7, 10 and 11 HPA events, respectively (see www.pik–potsdam.de/~petri/extr_2012_2013.html#movies, which presents time series of $\tilde{A}_{m,obs}$ for $m = 4$, 5, 6, 7, and 8 for May–September 1980–2013).

It is instructive to compare these numbers with those characteristic of a set of the years during 1979–2012 with no or only one major regional extreme event (in terms of land surface temperature and land precipitation anomalies) in the NH midlatitudes, from late April/early May to late September/early October, as reported yearly since 1993 in the World Meteorological Organization statements on the status of the global climate (see also ref. 38). According to www.pik–potsdam.de/~petri/extr_2012_2013.html#movies, out of this set of 10 y, the year 1981 saw the largest number, four, of HPA events for the waves with $m = 6$, 7, and 8 in total, and only one of those four events was preceded by a QRA event. These years are thus clearly linked to a near-absence of quasiresonant wave amplification.

Fig. 2 gives an example of a QRA–HPA event that began as a QRA event with 10 August 2012 as the central date, followed, with a lag of 5 d, by an HPA event during the strong heat waves in the western and eastern United States, accompanied by severe flooding in the central United States that occurred simultaneously with destructive flooding in central China and severe droughts in eastern and western China (44). The Fig. 2*A* shows a map of this HPA event. Fig. 2*B* plots the curve of the nondimensional stationary wave number $K_s^2a^2 = k^2 + l^2a^2$ (left y axis; see *Calculation of the Meridional Wave Number*) for the QRA event. Any points of intersection of this curve with the horizontal line $k = const$ in Fig. 2 mark the latitudinal position of the TP for the corresponding k wave, so that, in the case of two TPs, their abscissa specify the latitudinal positions of the waveguide's boundaries for the trapped k wave (*Calculation of the Meridional Wave Number*), provided the difference $K_s^2a^2 - k^2$ is positive between the TPs and all of the above-mentioned necessary conditions for QRA are met within the waveguide. In that case, $K_s^2a^2 - k^2$ yields the value of $l^2a^2 > 0$ within the waveguide (see *Calculation of the Meridional Wave Number*). Eq. **1a** then gives the value of the QRA amplitude $\tilde{A}_m$ of the forced m wave with m close to k. This situation is indeed found for the central date shown in Fig. 2 within the waveguide for the free wave with $k \approx 7.05$. The QRA amplitude $\tilde{A}_7 \approx (5.6 \pm 0.8)$ m·s^{-1} calculated by Eq. **1a** with the use of $\tilde{A}_7^{Or}$ derived from the temperature (41) and orography (46) data sets is close to the observed amplitude $\tilde{A}_{7,obs} \approx (5.4 \pm 1.3)$ m·s^{-1} reached in the following HPA event lagged by 5 d (see Fig. 1). Refer to *Estimation of the Error Bars* for a discussion of the error bars on these amplitudes. Notice that the observed amplitude of $m = 7$ for the central date of the QRA event (10 August 2012) was markedly lower than $\tilde{A}_7$ (see Fig. 1). This is characteristic of a number of the QRA–HPA events in May–September 2012 and 2013, where HPA event occurs about 5–15 d after the QRA event (in the 15-d running mean diagnostics used here).

Our second example is the central European flooding in May–June 2013, which was one of the strongest NH regional extremes (47). Its causal chain can be traced from autumn 2012, which featured record-low sea ice cover in the Arctic. This situation persisted into the winter 2012/2013, with high temperatures in the Arctic and very cold northern continents (48). Late snowmelt over the region in late April/early May, followed by heavy rains in late May/early June, resulted in extremely high water levels in the Danube, Elbe, and Rhine, with coastal flooding in early/middle June there (49). A strong snowmelt in late April/early May and torrential rains in late May/early June could have been caused by the occurrence of persistent quasibarotropic high-amplitude QRA structures with zonal wave numbers $m = 6$

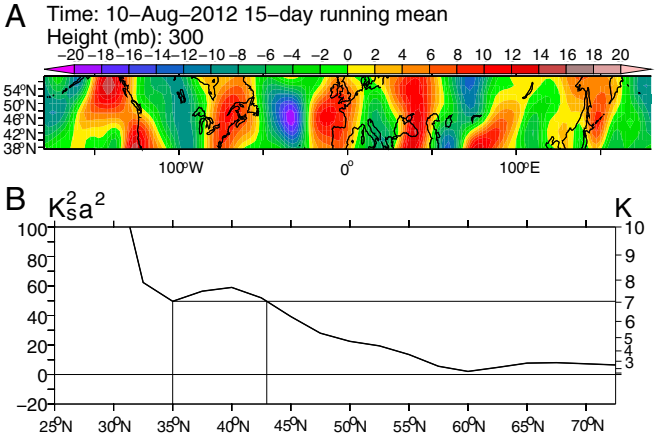

Fig. 2. The QRA event with 10 August 2012 as the central date, followed, with a lag of 5 d, by the observed HPA event during heat waves in the western and eastern United States and severe flooding in the central United States, accompanied by flooding in central China and droughts in eastern and western China (44). (*A*) Map (in meters per second) of the HPA event. (*B*) Nondimensional stationary wave number squared (the curve, left y axis) and resonance zonal wave number k (the straight line, right y axis) at the QRA event. All of the necessary conditions for the QRA event were met for the free wave with zonal wave number $k \approx 7.05$ within the midlatitude waveguide whose boundaries are marked by the vertical solid lines in *B*. The QRA amplitude $\tilde{A}_7 \approx (5.6 \pm 0.8)$ m·s^{-1} of the forced $m = 7$ component matches well the observed $\tilde{A}_{7,obs} \approx (5.4 \pm 1.3)$ m·s^{-1} for the HPA event lagged by 5 d (see Fig. 1).

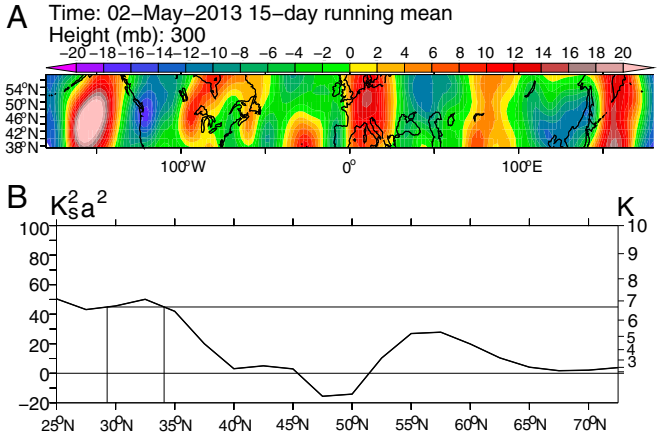

Fig. 3. The QRA event with 2 May 2013 as the central date during the catastrophic flood in central Europe. (*A*) Map (in meters per second) of the following observed HPA event for $m = 7$ with the central date shifted 1 d later. (*B*) Nondimensional stationary wave number squared (the curve, left *y* axis) and resonance zonal wave number *k* (the straight line, right *y* axis) at the QRA event. All of the necessary conditions for the QRA event were met for the free wave with zonal wave number $k \approx 6.8$ within the midlatitude waveguide whose boundaries are shown by the vertical solid lines in *B*. The QRA amplitude $\tilde{A}_7 \approx (4.4 \pm 0.6)$ m s^{-1} matches well the observed $\tilde{A}_{7,obs} \approx (4.5 \pm 1.3)$ m·s^{-1} of the following HPA event (see Fig. 1).

and $m = 7$ in the field of the NH midlatitude meridional velocity. The phase of these waves led to a northward flow over central Europe.

Fig. 3 illustrates one of these structures with $m = 7$ for 2 May 2013 as the central date of the QRA event. The HPA event peaked 1 d later. The necessary conditions for QRA were met for the quasistationary free wave with zonal wave number $k \approx 6.8$ within the midlatitude waveguide (see Fig. 3*B*). The QRA amplitude $\tilde{A}_7 \approx (4.4 \pm 0.6)$ m·s^{-1}, calculated by Eq. **1a** with the use of the forcing amplitude $\tilde{A}_7^{Ort}$ derived from refs. 41 and 46 data sets, matches well the observed amplitude $\tilde{A}_{7,obs} \approx (4.5 \pm 1.3)$ m·s^{-1} for the following HPA event (see Fig. 1). We note that a similar situation has been observed again during the devastating flood in southeastern Europe in May 2014 (50).

Discussion

Overall, the results of our calculations of the amplitudes of the waves with $m = 6$, 7, and 8 in the field of the midlatitude meridional velocity at 300 hPa suggest that 12 of the 17 HPA events during May–September of 2012 and 2013 substantially coincided or were preceded by QRA events up to 2 wk earlier (see Fig. 1). The QRA amplitudes calculated by Eqs. **1a** and **1b** match—with an accuracy of the order of 1 m·s^{-1}—the amplitudes of the observed HPA events. These results strongly suggest that, in spring-to-autumn 2012 and 2013, the QRA mechanism played an important role in generating HPA events for wave numbers $m = 6$, 7, and 8 that were accompanied by regional weather extremes, causing serious damage for society.

However, four occurrences of HPA events marked by open circles in Fig. 1 cannot be explained by the QRA mechanism. Also, in one case denoted by the open square in Fig. 1, QRA predicted an HPA event that did not happen. This attests that the QRA, as described here in a quasilinear approximation, is not, of course, the only mechanism for generating regimes of high-amplitude midlatitude waves with $m = 6$, 7, and 8. Other important competing mechanisms exist that can drive high-amplitude midlatitude extratropical planetary waves, like the Branstator mechanism (26), El Niño–Southern Oscillation (51), and North Atlantic Oscillation (NAO) (37). The choice of the mean flow and the scale separation between the mean flow and the stationary waves is critical. In our paper, we have dealt with the zonally averaged zonal winds as the mean flow and excluded from our consideration packets of quasistationary planetary waves trapped in predominantly meridional elongated waveguides, specifically those originating in the tropics. On the other hand, a large number of recent NH summer extremes occurred as circumglobal chains of alternating-in-longitude regional droughts and floods, embracing a large part of the midlatitude belt (see Figs. 2 and 3). A substantial part of these extremes could be favored by zonally elongated trains of the midtroposphere planetary waves (see, e.g., refs. 21, 34, and 38). In this paper, we investigated such wave trains with zonal wave numbers $m = 6$, 7, and 8, triggered by the QRA events. Our results showed that the time shift between the QRA event and respective HPA event could be up to about half a month. This is close to the "integral e-fold time scale" of excitation and decay of the persistent teleconnection anomalies observed over the North Pacific, North Atlantic, and Siberia sectors of the NH (52).

The QRA mechanism is considered in the present paper at the conceptual level: In the working equation for the azonal stream function, zonally averaged zonal flows and azonal forcing at the EBL are prescribed using observational data (refs. 41 and 46). For that reason, the QRA mechanism as discussed here is only a diagnostic, and not a predictive, theory of the zonally elongated planetary wave amplification.

As to the quasistationary planetary waves with $m = 4$ and $m = 5$ mentioned in the Introduction, a wave action of these waves can propagate far to the extratropics even under normal conditions (25, 42). In the present paper, we analyzed the May–September time series of the amplitudes of the observed waves with $m = 4$ and $m = 5$ over the 1980–2013 time range (www.pik–potsdam.de/~petri/extr_2012_2013.html#movies). The numbers of the HPA events for $m = 4$ and $m = 5$ were 16 and 20 in the first 11 y, 17 and 15 in the second 11-y period, and 20 and 25 in the last 12 y. The obtained results might indicate an increase in the number of such events for the waves with $m = 4$ and $m = 5$ in the last decade or so, compared with the previous ones, but this conclusion needs further verification.

Conclusions

We show that, in May–September 2012 and 2013, the majority (12 of 17) of HPA events, for midlatitude wave numbers $m = 6$, 7, and 8, with the observed amplitudes exceeding 1.5 SDs from the 1980–2013 May–September climatology, occurred when the resonance conditions for these wave numbers were fulfilled, within up to 2 wk preceding an HPA event. In all 12 cases, the wave amplitudes predicted by the QRA theory (Eqs. **1a** and **1b**) were in a good agreement with the observed amplitudes of the related HPA events, which favored strong regional weather extremes in the NH midlatitudes.

1. Intergovernmental Panel on Climate Change (2013) *Climate Change 2013: The Physical Science Basis. Contribution of Working Group I to the Fifth Assessment Report of the Intergovernmental Panel on Climate Change* (Cambridge Univ Press, Cambridge, UK).
2. World Meteorological Organization (2011) *Weather Extremes in a Changing Climate: Hindsight on Foresight* (World Meteorol Org, Geneva), Publ 1075.
3. Coumou D, Rahmstorf S (2012) A decade of weather extremes. *Nat Clim Chang* 2(7): 491–496.
4. Meehl GA, Tebaldi C (2004) More intense, more frequent, and longer lasting heat waves in the 21st century. *Science* 305(5686):994–997.
5. Coumou D, Robinson A, Rahmstorf S (2013) Global increase in record-breaking monthly-mean temperatures. *Clim Change* 118(3):771–782.
6. Coumou D, Robinson A (2013) Historic and future increase in the global land area affected by monthly heat extremes. *Environ Res Lett* 8(3):034018.
7. Westra S, Alexander LV, Zwiers FW (2013) Global increasing trends in annual maximum daily precipitation. *J Clim* 26(11):3904–3918.

8. Zhang X, Wan H, Zwiers FW, Hegerl GC, Min S-K (2013) Attributing intensification of precipitation extremes to human influence. *Geophys Res Lett* 40(19):5252–5257.
9. Lehmann J, Coumou D, Frieler K (2015) Increased record-breaking precipitation events under global warming. *Clim Change* 132(4):501–515.
10. Palmer TN (2013) Climate extremes and the role of dynamics. *Proc Natl Acad Sci USA* 110(14):5281–5282.
11. Orsolini YJ, Senan R, Benestad RE, Melsom A (2012) Autumn atmospheric response to the 2007 low Arctic sea ice extent in coupled ocean-atmosphere hindcasts. *Clim Dyn* 38(11):2437–2448.
12. Schär C, et al. (2004) The role of increasing temperature variability in European summer heatwaves. *Nature* 427(6972):332–336.
13. Luterbacher J, Dietrich D, Xoplaki E, Grosjean M, Wanner H (2004) European seasonal and annual temperature variability, trends, and extremes since 1500. *Science* 303(5663):1499–1503.
14. Tachibana Y, Nakamura T, Komiya H, Takahashi M (2010) Abrupt evolution of the summer Northern Hemisphere annular mode and its association with blocking. *J Geophys Res* 115(D12):D12125.
15. Black E, Blackburn M, Hoskins BJ, Methven J (2004) Factors contributing to the summer 2003 European heatwave. *Weather* 59(8):217–223.
16. Cassou C, Terray L, Phillips AS (2005) Tropical Atlantic influence on European heat waves. *J Clim* 18(15):2805–2811.
17. Hong C, Hsu H, Lin N, Chiu H (2011) Roles of European blocking and tropical-extratropical interaction in the 2010 Pakistan flooding. *Geophys Res Lett* 38(13):L13806.
18. Lau W, Kim KM (2012) The 2010 Pakistan flood and Russian heat wave: Teleconnection of hydrometeorological extremes. *J Hydrometeorol* 13(1):392–403.
19. Wang SY, Hipps LE, Gillies RR, Jiang X, Moller AL (2010) Circumglobal teleconnection and early summer rainfall in the US Intermountain West. *Theor Appl Climatol* 102(3): 245–252.
20. Schubert S, Wang H, Suarez M (2011) Warm season subseasonal variability and climate extremes in the Northern Hemisphere: The role of stationary Rossby waves. *J Clim* 24(18):4773–4792.
21. Teng H, Branstator G, Wang H, Meehl GA, Washington WM (2013) Probability of US heat waves affected by a subseasonal planetary wave pattern. *Nat Geosci* 6(12):1–6.
22. Feudale L, Shukla J (2011) Influence of sea surface temperature on the European heat wave of 2003 summer. Part I: An observational study. *Clim Dyn* 36(9):1691–1703.
23. Lupo AR, Smith PJ (1994) Climatological features of blocking anticyclones in the Northern Hemisphere. *Tellus Part A* 47(4):439–456.
24. Ogi M (2004) The summertime annular mode in the Northern Hemisphere and its linkage to the winter mode. *J Geophys Res* 109(D20):D20114.
25. Hoskins BJ, Karoly DJ (1981) The steady linear response of a spherical atmosphere to thermal and orographic forcing. *J Atmos Sci* 38(6):1179–1196.
26. Branstator G (2002) Circumglobal teleconnections, the Jet Stream Waveguide, and the North Atlantic Oscillation. *J Clim* 15(14):1893–1910.
27. Trenberth K, Fassullo J (2012) Climate extremes and climate change: The Russian heat wave and other climate extremes of 2010. *J Geophys Res* 117(D17):D17103.
28. Francis JA, Vavrus SJ (2012) Evidence linking Arctic amplification to extreme weather in mid-latitudes. *Geophys Res Lett* 39(6):L06801.
29. Cohen J, Jones J, Furtado JC, Tziperman E (2013) Warm Arctic, cold continents: A common pattern related to arctic sea ice melt, snow advance, and extreme winter weather. *Oceanography (Wash DC)* 26(4):150–160.
30. Coumou D, Lehmann J, Beckmann J (2015) Climate change. The weakening summer circulation in the Northern Hemisphere mid-latitudes. *Science* 348(6232):324–327.
31. Lehmann J, Coumou D (2015) The influence of mid-latitude storm tracks on hot, cold, dry and wet extremes. *Sci Rep* 5:17491.
32. Screen JA (2013) Influence of Arctic sea ice on European summer precipitation. *Environ Res Lett* 8(4):044015.
33. Hanna E, et al. (2014) Atmospheric and oceanic climate forcing of the exceptional Greenland ice sheet surface melt in summer 2012. *Int J Climatol* 34(4):1022–1037.
34. Petoukhov V, Rahmstorf S, Petri S, Schellnhuber HJ (2013) Quasiresonant amplification of planetary waves and recent Northern Hemisphere weather extremes. *Proc Natl Acad Sci USA* 110(14):5336–5341.
35. Coumou D, Petoukhov V, Rahmstorf S, Petri S, Schellnhuber HJ (2014) Quasi-resonant circulation regimes and hemispheric synchronization of extreme weather in boreal summer. *Proc Natl Acad Sci USA* 111(34):12331–12336.
36. Cohen J, et al. (2014) Recent Arctic amplification and extreme mid-latitude weather. *Nat Geosci* 7(9):627–637.
37. Hoskins B, Woollings T (2015) Persistent extratropical regimes and climate extremes. *Curr Clim Change Rep* 1(3):115–124.
38. Screen JA, Simmonds I (2014) Amplified mid-latitude planetary waves favour particular regional weather extremes. *Nat Clim Chang* 4(8):704–709.
39. Fraedrich K, Böttger H (1978) A wavenumber frequency analysis of the 500 mb geopotential at 50°N. *J Atmos Sci* 35(4):745–750.
40. Held IM (1983) Stationary and quasi-stationary eddies in the extratropical troposphere: Theory. *Large-Scale Dynamical Processes in the Atmosphere*, eds Hoskins BJ, Pearce RP (Academic, London), pp 127–168.
41. Kalnay E, et al. (1996) The NCEP/NCAR 40-year reanalysis project. *Bull Am Meteorol Soc* 77(3):437–471.
42. Haurwitz B (1940) The motion of atmospheric disturbances. *J Mar Res* 3:35–45.
43. Garcia RR (1991) Parameterization of planetary wave breaking in the middle atmosphere. *J Atmos Sci* 48(11):1405–1419.
44. World Meteorologial Organization (2013) *WMO Statement on the Status of the Global Climate in 2012* (World Meteorol Org, Geneva), Publ 1108.
45. World Meteorologial Organization (2014) *WMO Statement on the Status of the Global Climate in 2013* (World Meteorol Org, Geneva), Publ 1130.
46. Hastings DA, Dunbar PK (1999) *Key to Geophysical Records Documentation(KGRD) 34*, Global Land One-kilometer Base Elevation (GLOBE) Digital Elevation Model (DEM) (Natl Geophys Data Cent, Boulder, CO), Vol 1.0.
47. Hov Ø, et al. (2013) *Trends in Extreme Weather Events in Europe: Implications for National and European Union Adaptation Strategies* (Eur Acad Sci Advisory Counc, Halle, Germany), Policy Rep 22.
48. Slingo J (2013) *Why Was the Start to Spring 2013 So Cold?* (Met Off, Exeter, UK).
49. Van der Schrier G, et al. (2013) *Central European Flooding 2013*. Available at cib.knmi.nl/mediawiki/index.php/Central_European_flooding_2013. Accessed July 1, 2013.
50. Stadtherr L, Coumou D, Petoukhov V, Petri S, Rahmstorf S (2016) Record Balkan floods 2014 linked to planetary wave resonance. *Sci Adv* 2(4):e1501428.
51. Douville H, et al. (2011) Tropical influence on boreal summer mid-latitude stationary waves. *Clim Dyn* 37(9):1783–1798.
52. Feldstein SB (2000) The timescale, power spectra, and climate noise properties of teleconnection patterns. *J Clim* 13(24):4430–4440.
53. Charney JG, Eliassen A (1949) A numerical method for predicting the perturbations of the middle latitude westerlies. *Tellus* 1(2):38–54.
54. Pedlosky J (1979) *Geophysical Fluid Dynamics* (Springer, New York).
55. Uppala S, Simmons A, Dee D, Kållberg P, Thépaut J-N (2008) Atmospheric reanalyses and climate variations. Climate Variability and Extremes during the Past 100 Years, eds Brönnimann S, et al. (Springer, New York), pp 103–118.